Spectroscopic study of the E1Σ+g "shelf" state in 7Li2

R. A. Bernheim, L. P. Gold, C. A. Tomczyk, and C. R. Vidal

Citation: J. Chem. Phys. **87**, 861 (1987); doi: 10.1063/1.453293
View online: http://dx.doi.org/10.1063/1.453293
View Table of Contents: http://jcp.aip.org/resource/1/JCPSA6/v87/i2
Published by the AIP Publishing LLC.

Spectroscopic study of the $E\,^1\Sigma_g^+$ "shelf" state in $^7Li_2$

R. A. Bernheim, L. P. Gold, and C. A. Tomczyk[a)]
Department of Chemistry, The Pennsylvania State University, 152 Davey Laboratory, University Park, Pennsylvania 16802

C. R. Vidal
Max-Planck-Institut für Extraterrestrische Physik, D-8046 Garching, Federal Republic of Germany

(Received 10 December 1986; accepted 9 April 1987)

The $E\,^1\Sigma_g^+$ "shelf" state of the $^7Li_2$ molecule was investigated using a pulsed optical optical double resonance technique. The measurements cover the vibrational levels in the range $0 \leqslant v \leqslant 29$ including the shelf region around $13 \leqslant v \leqslant 15$. Molecular constants have been determined. Using an inverted perturbation approach, an effective potential energy curve has been generated within the adiabatic approximation whose quantum mechanical energy eigenvalues reproduce all the measured term values to within 0.113 cm^{-1} for the range $0 \leqslant v \leqslant 23$ and $0 \leqslant J \leqslant 47$.

I. INTRODUCTION

One of the first two-color pulsed optical–optical double resonance (OODR) experiments performed was carried out on the $^7Li_2$ molecule in 1979.[1] Since that time this powerful technique has been used to characterize nearly three dozen excited *gerade* states in the lithium dimer. These include the $E\,^1\Sigma_g^+$ state,[2] the $F\,^1\Sigma_g^+$ state,[3] the $G\,^1\Pi_g$ state[4] and three *gerade* Rydberg series.[5] One of these states, the $E\,^1\Sigma_g^+$, was found to exhibit an unusual potential well behavior. Extrapolating a Birge–Sponer plot of the spectroscopic data for the $v^* = 0$–12 vibrational levels resulted in a dissociation energy which was 5000 cm^{-1} below the closest pair of atomic states to which the $E\,^1\Sigma_g^+$ state could be correlated. The explanation advanced for this extremely unusual behavior was the possibility of a double minimum potential well such as the well-known $E,F\,^1\Sigma_g^+$ state of H_2 [6,7] or the recently observed $(2)\,^1\Sigma_u^+$ state of Na_2.[8,9] Independently, *ab initio* calculations by Konowalow and Fish revealed a double minimum potential for this state with the outer well depth being a scant 30 cm^{-1} deep.[10,11] This result nicely corroborated the explanation of the experimental results for the lower, inner part of the potential well and the unusual Birge–Sponer extrapolation. The present work reports a thorough investigation of the transition region between the narrow, lower part of the potential and the wide, upper region. Instead of an outer well a broad "shelf" region was found with no intermediate barrier maximum. This finding agrees also with more recent *ab initio* calculations by Schmidt-Mink *et al.*[12]

An analysis of the spectroscopic data in terms of a Dunham-type expansion turned out to be very unsatisfactory because as many as 24 coefficients had to be used to reproduce the measurements. Attempts to find an RKR potential based on these molecular constants resulted in a nonphysical behavior for the portion of the potential energy curve above the shelf region.[13] In general an RKR method works most successfully for generating potential energy curves of a moderately anharmonic oscillator, and it cannot be applied to a potential well with an unusual shape such as a double minimum or shelf potential.

An alternative, more powerful method of calculating potential energy curves from experimental data is the inverted perturbation approach (IPA).[14–16] In the past this method has been successfully applied to several cases where the RKR method has worked very poorly or has failed completely as, for example, the $A\,^1\Sigma^+$ and $B\,^1\Pi$ states of LiH.[17,18] It will be shown that an application of the IPA method to the $E\,^1\Sigma_g^+$ shelf state of the lithium dimer yields a better potential energy curve.

II. EXPERIMENTAL

In the OODR experiment, two independently tunable pulsed dye lasers are used to pump the $^7Li_2$ molecules from a given rovibronic level (v'',J'') in the molecular ground state to a rovibronic level (v^*,J^*) in the $E\,^1\Sigma_g^+$ state. The transitions take place via a real rovibronic level (v',J') in an intermediate state of the molecule. In this case the intermediate state is the $A\,^1\Sigma_u^+$ state.

The experimental apparatus, which has been previously described in detail,[2–5] includes a Molectron UV-1000 nitrogen laser which pumps two Hänsch-type dye lasers. The first or pump dye laser is set at a fixed wavelength to excite $^7Li_2$ molecules from a (v'',J'') level of the ground state to a known (v',J') level in the $A\,^1\Sigma_u^+$ state.[19] The second or probe dye laser is then scanned to produce a subsequent excitation of molecules from the (v',J') level of the intermediate $A\,^1\Sigma_u^+$ state to the final (v^*,J^*) levels of the $E\,^1\Sigma_g^+$ state.

From the $E\,^1\Sigma_g^+$ state, radiative transitions can occur either to the $A\,^1\Sigma_u^+$ state or to the $B\,^1\Pi_u$ state. Both states can then undergo transitions to the ground state by emitting light in the 390–590 nm region. A color filter is used with a 1P28 photomultiplier tube to monitor this fluorescence. Some OODR transitions may be excited by absorption of two probe laser photons. These unwanted features are eliminated as described previously[4] with the remaining observed spectrum being due to absorption of one photon each from the pump and probe lasers.

[a)] Present address: PPG Industries, Inc., P. O. Box 11472, Pittsburgh, PA 15238.

 0021-9606/87/140861-08$02.10

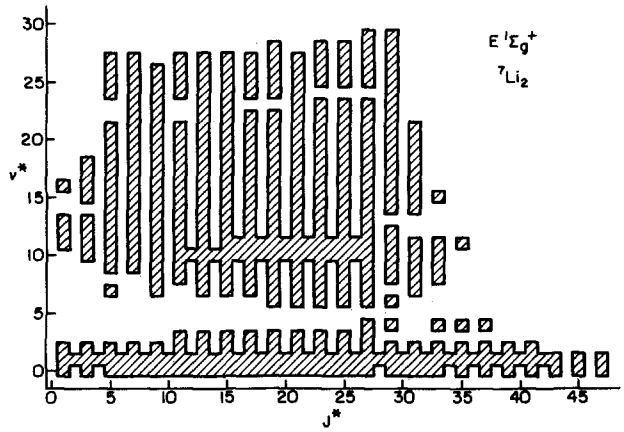

FIG. 1. Data field showing the rovibronic levels covered by the OODR observations on the $E\,^1\Sigma_g^+$ state of $^7Li_2$.

The probe laser wavelength is measured using neon and argon optogalvanic cells together with interference fringes from a Fabry–Perot interferometer having a free spectral range of 0.8 cm^{-1}.

The OODR signal, the optogalvanic signal, and the interferometer fringes are all recorded on a strip chart recorder and digitally using an Apple II^+ microcomputer. The Apple II^+ microcomputer is interfaced with the signal detection electronics via analog to digital converters and parallel data buffers.[20] The OODR spectral line positions are measured with an accuracy of $\pm$ 0.2 cm^{-1} using dye laser linewidths of 0.3 cm^{-1}. In a typical experiment both the pump and probe dye lasers are operated in the 660–760 nm range using mixtures of DCM in DMSO and ethanol.

The pump transitions were carefully chosen to exploit the method of combination differences for assigning the unusually complex OODR spectra which result from transitions to levels above $v^* = 12$ in the $E\,^1\Sigma_g^+$ state. Data were collected at helium buffer gas pressures of 70 and 23 Torr with the cell operating at a temperature of 800 °C. The use of two buffer gas pressures produced different amounts of collisional relaxation in the intermediate state which made it possible to unambiguously assign the rotational quantum numbers.[13] The relative intensities of the probe transitions originating from rotational levels that are directly pumped with respect to those originating from rotational levels that are populated by collisional transfer, are different at different buffer gas pressures.

In the present experiments a total of 1922 transitions were measured in the region $0 \leqslant v^* \leqslant 29$.

III. RESULTS AND SPECTRAL ANALYSIS

The data field of measured (v^*, J^*) levels in the $E\,^1\Sigma_g^+$ state as determined from both the previous[2] and the present experimental studies is shown in Fig. 1. Mostly odd J^* levels were measured in the $E\,^1\Sigma_g^+$ state because the 3/2 nuclear spin value of ^7Li gives a 5:3 population ratio for odd:even rotational levels of the ground state.[21] This results in stronger, more easily detected transitions from the odd J'' ground state levels, making these transitions more favorable pump line choices. Only odd J^* levels in the $E\,^1\Sigma_g^+$ state can be populated from odd J'' levels in the ground state.

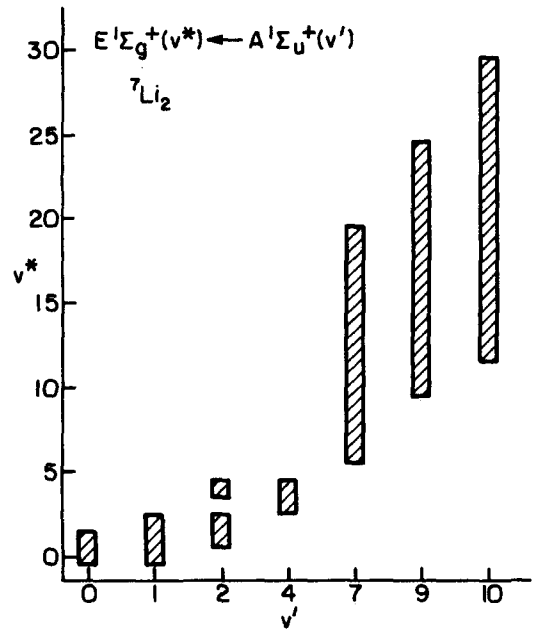

FIG. 2. The range of vibrational levels v^* used for determining the energy level structure of the $E\,^1\Sigma_g^+$ state of $^7Li_2$ using different (v', J') levels of the intermediate $A\,^1\Sigma_u^+$ state.

Figure 2 shows the data field of v^* levels in the $E\,^1\Sigma_g^+$ state which were excited from the various v' levels pumped in the intermediate $A\,^1\Sigma_u^+$ state. Overlapping measurements for the levels with $v^* \geqslant 13$ were obtained in order to use combination differences for assigning the unusually complex OODR spectra in this region.

An example of a typical OODR scan for the region $v^* = 9$–12 is shown in Fig. 3. This scan contains four separate bands in a 450 cm^{-1} wide energy region. In contrast, the more complex, highly overlapped spectra obtained beyond $v^* = 12$ are shown in Fig. 4. In particular, there are four overlapped bands in the region of the $v^* = 13$ bandhead at approximately 13 275 cm^{-1}, making this spectral region particularly congested.

The two different theoretical calculations which have so far been performed to obtain the basic spectroscopic constants and the potential energy curves for the $E\,^1\Sigma_g^+$ state, also predict the position of the vibrational energy levels.[10–12] The vibrational energy levels for the experiment based on extrapolated values for the levels with $J^* = 0$, are given in Table I together with the values obtained by the two *ab initio* calculations. There appears to be better agreement between the experiment and the calculations of Schmidt-Mink *et al.*[12] especially in the region around $v^* = 13$–15. The calculation of Konowalow and Fish[10,11] predicts the minimum $\Delta G(v)$ value to occur for $v^* = 13$–14, while experiment and the calculations of Schmidt-Mink *et al.*[12] predict the minimum $\Delta G(v)$ value to occur for $v^* = 14$–15. Konowalow and Fish also predict the existence of an extra vibrational energy level. All three sets of values (two theoretical plus our experimental) agree well in the $v^* = 0$–12 region. The $v^* = 13$ level of Konowalow and Fish does not match to an experimentally measured level or to a level calculated by Schmidt-Mink *et al.*[12] The vibrational level numbering differs therefore by one

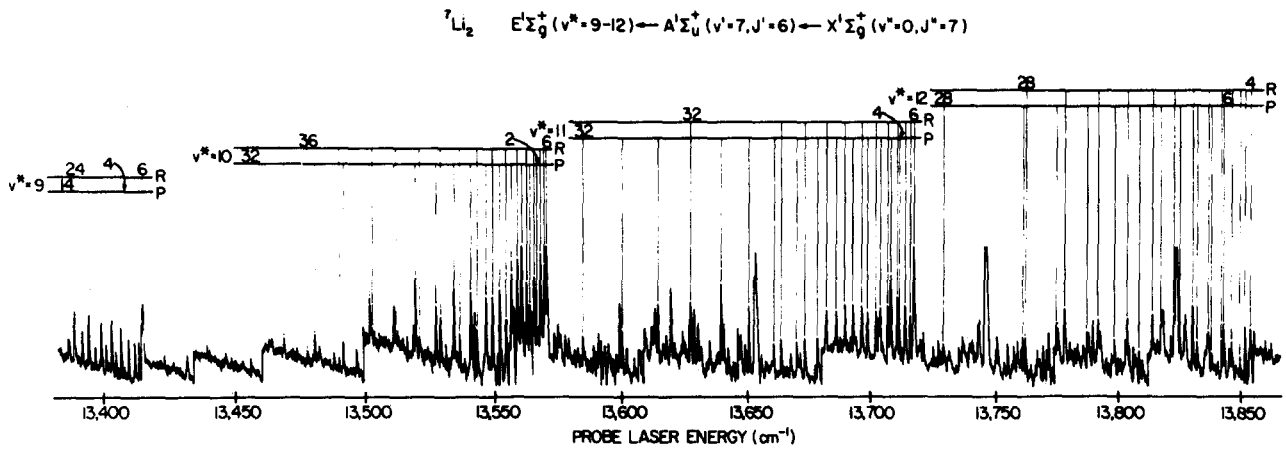

FIG. 3. Detected OODR spectrum for the $v^* = 9$–12 region of the $E\,^1\Sigma_g^+$ state of $^7Li_2$ showing the slight overlap between vibrational bands in this region. The helium buffer gas pressure was 70 Torr with the cell operating at a temperature of about 800 °C.

unit beyond $v^* = 13$ for the calculations of Konowalow and Fish compared to the experiments and the values of Schmidt-Mink *et al.*[12] Also the calculations of Konowalow and Fish predict a shallow outer minimum, whereas the calculations of Schmidt-Mink *et al.* show the region to be a shelf.

IV. MOLECULAR CONSTANTS

The measured line positions $\bar{\nu}$ of the probe transitions from the $E\,^1\Sigma_g^+ - A\,^1\Sigma_u^+$ system are given by

$$\bar{\nu} = T(v^*,J^*) - T(v',J'), \tag{1}$$

where for a $^1\Sigma$ state the term values are usually described by a Dunham expansion of the form

$$T(v,J) = \sum_{j,k} Y_{jk}\,[v + 1/2]^j [J(J+1)]^k. \tag{2}$$

Because of the unusual shape of the $E\,^1\Sigma_g^+$ potential energy curve, a straightforward global least-squares fit of the measured line positions turned out to be unsatisfactory[13] and a different method for determining the molecular constants was chosen. Since the term values $T(v',J')$ of the intermediate $A\,^1\Sigma_u^+$ state have already been accurately measured by Kusch and Hessel[19] with a standard error of 0.01 cm^{-1} covering all the relevant pump levels in our experiment, we added their measured term values $T(v',J')$ of the $A\,^1\Sigma_u^+$ state to our measured line positions $\bar{\nu}$ and obtained the term values $T(v^*,J^*)$ of the $E\,^1\Sigma_g^+$ state[22] according to Eq. (1). The experimental errors of Kusch and Hessel are about an order of magnitude smaller than the errors of our OODR measurements. Hence no additional errors are introduced into the analysis of the term values of the $E\,^1\Sigma_g^+$ state.

In the process of determining the molecular constants of the $E\,^1\Sigma_g^+$ state from a global least-squares fit of the measured term values, it was found that many centrifugal distortion terms are required which are due to the large anharmonicity of the potential energy curve in the region of the shelf. As a result, one obtains molecular constants whose physical significance is somewhat obscure. It proved most advantageous to subdivide the entire data field of the $E\,^1\Sigma_g^+$ state into three regions. Region I covers all term values below the shelf with $0 \leqslant v^* \leqslant 12$. Region II contains the shelf region with $13 \leqslant v^* \leqslant 15$ and region III finally covers all the remaining term values above the shelf with $16 \leqslant v^* \leqslant 29$. Since regions I

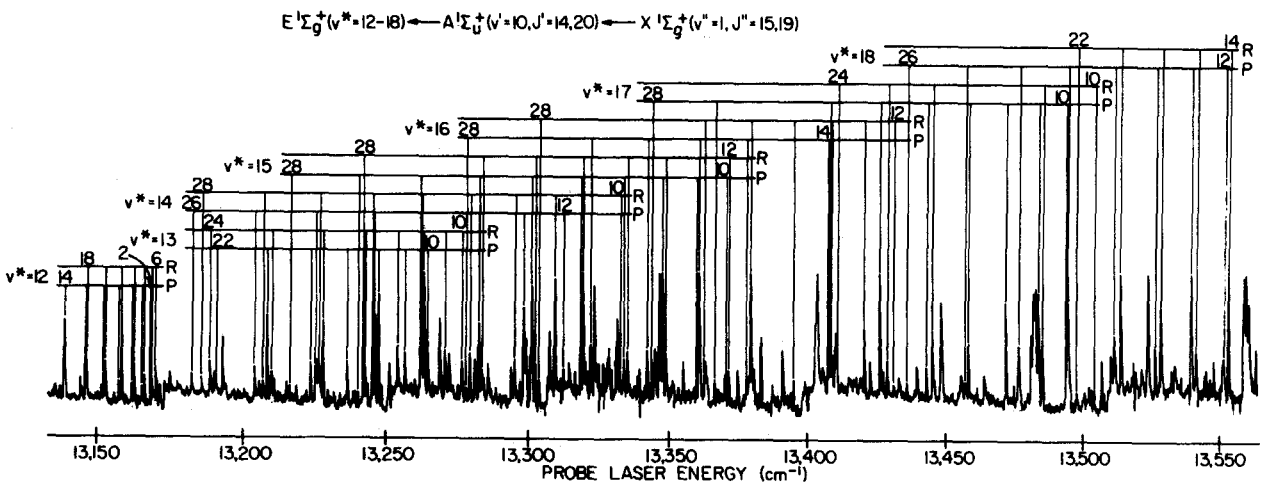

FIG. 4. Detected OODR spectrum for the region around $v^* = 13$ of the $E\,^1\Sigma_g^+$ state of $^7Li_2$ showing a severe overlap of vibrational bands in this region. The helium buffer gas pressure was 70 Torr with the cell operating at a temperature of about 800 °C.

TABLE I. Comparison between the experimental G_v and the theoretical values as given by Konowalow and Fish (KF) (Refs. 10 and 11) and by Schmidt-Mink, Müller, and Meyers (SMM) (Ref. 12) for the $E\,^1\Sigma_g^+$ state of $^7Li_2$. COmparison is made for $J=0$ and all values are given in cm^{-1}.

v	Exper. G_v	Theor. G_v (SMM)	Exper. G_v $-G_v$ (SMM)	Theor. G_v (KF)	Exper. G_v $-G_v$ (KF)
0	122	123	−1	123	−1
1	360	362	−2	364	−4
2	588	591	−3	595	−7
3	804	808	−4	815	−11
4	1008	1015	−7	1024	−16
5	1201	1211	−10	1222	−21
6	1386	1399	−13	1410	−24
7	1564	1579	−15	1590	−26
8	1734	1752	−18	1761	−27
9	1898	1918	−20	1924	−26
10	2055	2077	−22	2077	−22
11	2202	2225	−23	2219	−17
12	2338	2359	−21	2344	−6
13	2455	2473	−18	2416	+39
14	2524	2553	−29	2450	+74
15	2567	2603	−36	2506	+61
16	2627	2661	−34	2566	+61
17	2691	2725	−34	2630	+61
18	2759	2794	−35	2699	+60
19	2830	2866	−36	2770	+60
20	2904	2941	−37	2844	+60
21	2980	3018	−38	2921	+59
22	3058	3096	−38	2998	+60
23	3137	3177	−40	3078	+59
24	3216	3259	−43	3159	+57
25	3297	3342	−45	3241	+56
26	3380	3426	−46	3325	+55
27	3464	3512	−48	3409	+55
28	3549	3598	−49	3494	+55
29	3634	3684	−50	3580	+54

and III behave very much like normal anharmonic oscillators they require a rather small number of centrifugal distortion terms. For region I the lowest order Dunham-type coefficients obey rather well the Kratzer relation,[21] $D_e = 4B_e^3/\omega_e^2$. This is very useful for finding the intial potential energy curve for the IPA method as explained below. Furthermore, the value for T_e for the $E\,^1\Sigma_g^+$ state can be taken from the effective value $(Y_{00}^*)_{\text{eff}} = 27\,409.42\ cm^{-1}$ of region I in Table I which according to Vidal[16] is given by

$$(Y_{00}^*)_{\text{eff}} = T_e + Y_{00}^*. \tag{3}$$

$Y_{00}^* = -0.811\ cm^{-1}$ is the Dunham coefficient derived below in the IPA procedure which refers all term values of the $E\,^1\Sigma_g^+$ state to the minimum of the potential energy curve. It should also be noted that the Dunham-type coefficients of region I differ somewhat from the constants given by Bernheim *et al.*[2] although the same data field was used in both investigations. The reason for this is that a few more Dunham-type coefficients and more measurements were employed in the present analysis.

Our final sets of Dunham-type coefficients for the three different regions of the data field are summarized in Table II. These molecular constants reproduce the measured term values within their standard errors. In regions I, II, and III we obtained a total standard error of 0.1094, 0.0899, and 0.0662 cm^{-1}, respectively. A larger number of centrifugal distortion constants is required in the shelf region II. Since three different v^* values are contained in the data field of the shelf region II, just as many Dunham-type expansion coefficients with respect to v^* had to be used for describing the anharmonicity in the transition region.

The molecular constants are given together with their standard errors in brackets which are given in units of the last digit of the molecular constant. In some cases a rather large number of digits had to be given in order to avoid any roundoff errors and to reproduce the measured term values. The reason for this is strong correlations among several adjacent molecular constants.[23]

In performing the least-squares fit of the three different regions, approximately 4% of the measured spectral transitions were removed that resulted in term values that differed by more than three standard errors of the measurements. However, most of the eliminated measurements were redundant ones, with the resulting term values determined by other line positions. All measured spectral line positions and term values are included in Ref. 22. In summary, 1085 transitions were used to determine 219 term values defining region I with $0 \leqslant v \leqslant 12$, 253 transitions for 41 term values in region II with $13 \leqslant v \leqslant 15$, and 501 transitions for 158 term values in region III with $16 \leqslant v \leqslant 29$.

V. POTENTIAL ENERGY CURVE

The unusual shape of the $E\,^1\Sigma_g^+$ potential energy curve is known to be due to an avoided curve crossing of the zero

TABLE II. Dunham-type coefficients of the $E\,^1\Sigma_g^+$ state given in cm^{-1}. The standard errors in brackets are given in units of the last digit and the following numbers are the exponents of 10 in the multiplying factor.

	Region I ($0 \leq v^* < 12$)			
$Y_{i,k}$	0	1	2	3
0	27409.42(17)	0.50473(19)	−7.76(12) − 6	−2.23(33) − 10
1	248.916(577)	−1.042(49) − 2	−1.10(21) − 6	
2	−6.6326(6290)	1.141(430) − 3	4.4(13) − 7	
3	1.30312(31093)	−1.146(177) − 3	−1.45(30) − 7	
4	−5.2087(8018) − 1	3.161(374) − 4	2.01(28) − 8	
5	9.63725(116333) − 2	−4.004(417) − 5	−9.17(89) − 10	
6	−8.98895(96174) − 3	2.441(232) − 6		
7	4.20192(42400) − 4	−5.835(507) − 8		
8	−7.9218(7749) − 6			

	Region II ($13 \leq v^* < 15$)				
$Y_{i,k}$	0	1	2	3	4
0	26391.31(1083)	12.6554(2170)	2.1369(1296) − 2	−6.79(31) − 5	3.58(25) − 8
1	432.437(1493)	−1.68292(2973)	−2.9652(1760) − 3	9.33(41) − 6	−4.93(34) − 9
2	−12.97275(5132)	5.6868(1016) − 2	1.0233(596) − 4	−3.20(14) − 7	1.69(11) − 10

	Region III ($16 \leq v^* < 29$)		
$Y_{i,k}$	0	1	2
0	32109.16(27436)	−2.35(25) − 1	1.21(13) − 4
1	−622.6881(761471)	6.904(468) − 2	−1.575(192) − 5
2	63.18777(874697)	−3.721(327) − 3	6.676(897) − 7
3	−3.187082(532382)	8.81(103) − 5	−9.36(138) − 9
4	9.371406(1811220) − 2	−7.77(121) − 7	
5	−1.499745(326663) − 3		
6	1.0126(2441) − 5		

order covalent and ionic potential energy curves which gives rise not only to the $E\,^1\Sigma_g^+$, but also to the $F\,^1\Sigma_g^+$ state.[10–12] It is this particular character of the potential energy curves which also necessitates a different approach for determining its shape. Since a semiclassical first-order WKB method, such as the well-known RKR method, is incapable of dealing with a shelf-type potential energy curve in a satisfactory manner, we applied the inverted perturbation approach. The objective of the IPA method is to generate a potential energy curve whose quantum mechanical energy eigenvalues agree in a least-squares sense with the measured term values. The IPA method is therefore a fully quantum mechanical procedure which has so far been based upon a rotating vibrator Hamiltonian.[16]

Initially the potential energy curve of region I with $0 \leq v^* < 12$ was investigated. In this region the $E\,^1\Sigma_g^+$ state behaves very much like a slightly anharmonic oscillator for which one can easily calculate an RKR potential.[2] Applying the IPA method to this part of the potential yielded only a minor improvement, indicating that the quantum mechanical corrections to the initial semiclassical RKR potential of region I are very small.

The situation changed quite dramatically when we tried to incorporate the shelf region II with $13 \leq v^* < 15$. In this case there was no direct way of obtaining a good initial potential for the shelf region from an RKR procedure. Instead we used the *ab initio* calculations[10–12] as a guide for finding a reasonable shape of the shelf region. For the correction function which improves the potential energy curve from one iteration to the next, a linear combination of Legendre polynomials has so far been used in most applications.[16] For our present problem, however, this is not an adequate correction function because region I requires only a very small correction, whereas the outer turning points of region II require a very large correction. Such a situation, where a localized large correction to the potential energy curve is required, cannot be well described by a linear combination of Legendre polynomials. To overcome this problem we started with several test runs in which we modified and improved the initial potential energy curve describing the shelf region by trial and error until the linear combination of Legendre polynomials became an adequate correction function which was able to handle the entire range of internuclear distances.

Having adjusted all the term values with $v^* < 15$ we finally extended the data field of the IPA method beyond the shelf region II into region III. To find a reasonable starting potential for the IPA method we proceeded in the following manner: Table II shows that region III, like region I, is well described by a slightly anharmonic oscillator for which an RKR potential can be constructed. Taking the outer turning points of the latter potential, a continuation of the previous potential energy curve was obtained. Since the inner turning points showed a small, but unphysical offset from the inner turning points of regions I and II, we determined the initial inner turning points instead from an exponential extrapolation of the potential energy curve of region I.

Even with this starting potential, the IPA method did not immediately provide a good potential covering all the measured term values. We therefore went again through a similar series of test runs in which we gradually improved

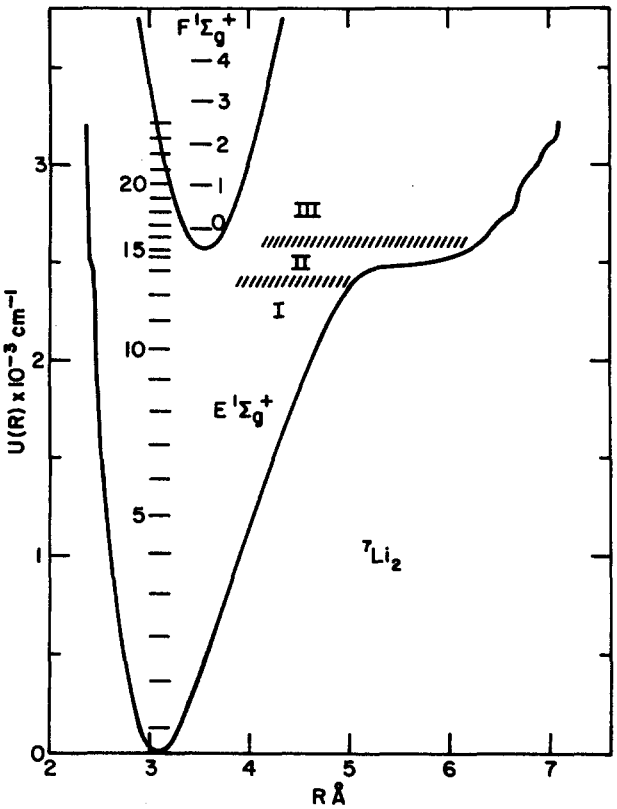

FIG. 5. Potential energy curves for the $E\,^1\Sigma_g^+$ and the $F\,^1\Sigma_g^+$ states of $^7Li_2$ which have been obtained within the adiabatic approximation. The experimentally determined vibrational energy levels and the IPA potential of the $E\,^1\Sigma_g^+$ state for $J = 0$ are given showing in particular the shelf region and the small irregularities arising from nonadiabatic contributions which are effectively hidden in our adiabatic approach.

TABLE III. Effective adiabatic potential energy curve of the $E\,^1\Sigma_g^+$ state.

n	G_v(cm^{-1})	R_{min}(Å)	R_{max}(Å)	B_v(cm^{-1})
0	122.17	2.903 689	3.300 763	0.499 634
1	360.10	2.787 885	3.486 965	0.488 968
2	587.58	2.715 507	3.636 818	0.476 847
3	803.49	2.660 709	3.776 433	0.463 629
4	1007.77	2.618 956	3.911 687	0.450 025
5	1201.48	2.585 122	4.043 602	0.436 735
6	1386.25	2.550 643	4.171 613	0.424 275
7	1563.54	2.512 628	4.295 685	0.412 747
8	1734.20	2.495 246	4.417 558	0.401 630
9	1898.20	2.485 062	4.540 225	0.390 136
10	2054.76	2.477 217	4.667 508	0.377 354
11	2202.34	2.470 272	4.806 349	0.361 986
12	2338.01	2.463 300	4.966 262	0.341 317
13	2454.65	2.449 606	5.196 422	0.303 435
14	2523.93	2.392 452	6.050 615	0.203 344
15	2567.19	2.391 872	6.218 782	0.228 781
16	2627.20	2.391 071	6.385 858	0.228 912
17	2690.81	2.390 221	6.475 745	0.232 929
18	2758.95	2.389 306	6.631 959	0.235 628
19	2830.23	2.388 337	6.697 453	0.237 305
20	2904.09	2.387 314	6.742 754	0.237 448
21	2979.79	2.386 238	6.865 527	0.238 259
22	3057.89	2.385 086	6.922 223	0.239 364
23	3137.47	2.383 854	7.057 533	0.236 792
24	3215.97	2.382 557	7.092 253	0.231 867

the initial starting potential until the fine adjustment could be taken care of by the linear combination of Legendre polynomials. From one series of test runs to the next it was advantageous to add only one new vibrational level at a time to the data field. This allows one to improve the potential energy curve in small parts. Admittedly this was a somewhat cumbersome procedure which strongly suggests the need for a different type of correction function in the IPA procedure. As an alternative correction function which has the desired flexibility, it appears that a cubic spline function[24] might be more powerful, and work on this is in progress.

Finally, we succeeded in generating a potential energy curve which is shown in Fig. 5 and is listed in Table III. Its quantum mechanical energy eigenvalues describe *all* measured term values for $v^* < 24$ and all J within a standard error of 0.113 cm^{-1}. This value is comparable to the standard error obtained in the initial least-squares fit of the measured term values as described in the previous section. Going beyond $v^* = 23$ did at this stage not appear to be worthwhile for the reasons explained below.

The standard error of the present IPA result has to be compared with earlier results[16] where it was found that by describing the measured term values by a Dunham-type expansion, the standard error of the IPA method was typically half as large as the standard error obtained from the least-squares fit of the measured line positions. This was generally due to the fact that the initial least-squares fit of the measured line positions has the tendency to remove part of the "noise" in the data and pretends a better definition of the measured term values. This situation holds, for example, also for the region I of our present analysis.

In the present case where, finally, the standard errors of the least-squares fit and of the IPA method for $v^* < 24$ become comparable, the IPA error might appear to be somewhat large. However, this is not the case. In view of the fact that we have made an adiabatic approximation for describing the effective potential energy curve which is based on a rotating vibrator Hamiltonian,[16] the small IPA error is actually rather surprising. The sharp bend of the outer turning points before the potential energy curve approaches the shelf, indicates a rather sudden change in the character of the electronic part of the wave function which is associated with the avoided curve crossing. This strongly suggests significant nonadiabatic contributions which have been considered, for example, by Dressler and co-workers[25,26] for the $E,F\,^1\Sigma_g^+$ state of H_2 and which have not yet been taken into account in our present analysis. Hence it appears that our effective, seemingly adiabatic potential energy curve has absorbed a significant portion of the nonadiabatic contributions.

In view of the expected nonadiabatic contributions one may wonder whether electronically coupled diabatic states or nuclear moment coupled adiabatic states form the more appropriate basis for describing the $E\,^1\Sigma_g^+$ and the $F\,^1\Sigma_g^+$ states of the $^7Li_2$ molecule. In this context Dressler[27] has introduced a very useful adiabaticity parameter γ which is defined by

$$\gamma = \frac{H_{el}}{\hbar \bar{\nu}_N}, \tag{4}$$

where $H_{el}/\hbar$ characterizes an electronic resonance frequency and ν_N the nuclear vibration frequency. The adiabaticity parameter distinguishes between the diabatic limit ($\gamma \ll 1$) and the adiabatic limit ($\gamma \gg 1$). For a weakly avoided curve crossing with $\gamma \ll 1$, the electronic resonance frequency is too small to permit the electrons to switch from one adiabatic state to the other while the nuclei vibrate through the region of the avoided curve crossing. In this limit, the nuclei prefer to follow the diabatic potential energy curves. In the opposite limit of a strongly avoided curve crossing with $\gamma \gg 1$, the nuclear vibration frequency is now so small that the electrons effectively resonate between the diabatic states and assume the properties of the adiabatic states while the nuclei vibrate through the region of the avoided curve crossing. In this limit the nuclei therefore prefer to follow the adiabatic potential energy curves.

Following Dressler,[27] H_{el} was estimated from the minimum energy separation between the adiabatic $E\,^1\Sigma_g^+$ and the $F\,^1\Sigma_g^+$ states near the avoided curve crossing which according to Fig. 5 amounts to 1900 cm^{-1}. For $\bar{\nu}_N$, the lowest vibrational frequency of 222.5 cm^{-1} from the upper adiabatic state, the $F\,^1\Sigma_g^+$ state, was taken.[3] In this manner one obtains an adiabaticity parameter $\gamma = 8.5$, which is well into the adiabatic regime with a strongly avoided curve crossing.

Even though our situation is expected to be well within the domain of the adiabatic limit, our adiabatic analysis certainly reveals some remaining difficulties, which are associated with generating an effective adiabatic potential energy curve. A careful inspection of the inner and outer turning points of this IPA potential curve around and above the shelf region revealed, on the present level of experimental accuracy, very small irregularities which hardly show up in Fig. 5. Since these irregularities occur in the vicinity of the minimum of the $F\,^1\Sigma_g^+$ state their origin has to be clearly associated with the nonadiabatic terms. A similar situation was previously encountered for the $E,F\,^1\Sigma_g^+$ state of H_2 with an adiabaticity parameter $\gamma \approx 2$. In their Fig. 1(a), Dressler *et al.*[26] have shown the energy difference between the measured term values and their adiabatic calculations.[7] Below the minimum of the $G,K\,^1\Sigma_g^+$ state these differences increase gradually with increasing energy, whereas above the minimum of the $G,K\,^1\Sigma_g^+$ state the energy difference shows large irregular fluctuations which are due to the vibronic coupling whose magnitude strongly depends on the particular phase of the vibronic wave functions of the $E,F\,^1\Sigma_g^+$ and the $G,K\,^1\Sigma_g^+$ states which rapidly changes from one vibrational level to the next. The large fluctuations have been well accounted for by Dressler *et al.*[26] in their Fig. 1(b).

In our present case, the small irregularities in regions II and III clearly indicate the nonadiabatic contributions, whereas in region I the nonadiabatic contributions grow smoothly and can easily be hidden in a purely adiabatic analysis. Since the phase of the vibronic wave functions inside the vibronic coupling terms is rather insensitive to the centrifugal term of the rotating vibrator Hamiltonian, an effective, adiabatic potential energy curve is therefore expected to account for the entire data field including *all J*.

A similar situation was recently also encountered for the $X\,^1\Sigma^+$ and the $A\,^1\Sigma^+$ state of the lithium hydrides where the adiabatic calculations of Bishop and Cheung[28,29] showed a systematic difference from the analysis of Vidal and Stwalley.[17] Bishop and Cheung have argued that the adiabatic analysis of Vidal and Stwalley apparently contains nonadiabatic contributions which are responsible for the differences between the measured term values and the adiabatic calculations. In view of our present results this explanation appears to be correct because the differences are larger than the accuracy of the calculations and of the spectroscopic analysis.

Despite the still existing deficiencies, an important result of the effective adiabatic potential is that it strongly supports the vibrational assignment of the OODR spectra in the vicinity of the strongly congested shelf region shown in Fig. 4. A shallow outer minimum as calculated by Konowalow and Fish[10,11] would not be able to provide the self-consistency of the measured term values as verified by the IPA method,[30] whereas the calculations of Schmidt-Mink *et al.*[12] are in reasonable agreement with our results. In order to explore the influence of the nonadiabatic contributions it would be highly desirable to have accurate measurements of the Franck–Condon factors or of the lifetimes in the vicinity of the shelf region. The significant influence of nonadiabatic terms on the lifetimes of the $E,F\,^1\Sigma_g^+$ state of H_2 was recently shown by Glass-Maujean *et al.*[31]

It also must be pointed out that the standard error of the IPA results was found to increase gradually as the data field was enlarged to higher v^* which is most likely due to the neglect of nonadiabatic terms. For this reason we stopped at $v^* < 24$ where the standard errors of the least-squares fit and of the IPA method became comparable. In this manner we certainly covered the entire shelf region which was of prime interest in our present analysis.

On the basis of an adiabatic analysis this paper has provided a detailed study of the $E\,^1\Sigma_g^+$ state, in particular around the shelf region. However, it also has become very clear where more work is needed. First of all, the IPA method has to be improved for handling highly anomalous potential energy curves such as double minimum or shelf potentials. This may be done by incorporating a more fiexible correction function such as a cubic spline function. In addition, a detailed analysis of the nonadiabatic effects of the $E\,^1\Sigma_g^+$ state has to be performed whose magnitude could be tested directly by measuring the Franck–Condon factors or the lifetimes. Such an analysis would require *ab initio* calculations which provide the vibronic coupling matrix between the $E\,^1\Sigma_g^+$ and the $F\,^1\Sigma_g^+$ states of the $^7Li_2$ molecule similar to the $E,F\,^1\Sigma_g^+$ and $G,K\,^1\Sigma_g^+$ states of the H_2 molecule.

ACKNOWLEDGMENTS

The authors are very grateful to Dr. K. Dressler for many helpful discussions. The authors also wish to acknowledge Mr. Doug Miller for his considerable help with the experiments. Support by the National Science Foundation and the Donors of the Petroleum Research Fund of the American Chemical Society is also gratefully acknowledged.

[1]R. A. Bernheim, L. P. Gold, P. B. Kelly, C. Kittrell, and D. K. Veirs, Phys. Rev. Lett. **43**, 123 (1979).
[2]R. A. Bernheim, L. P. Gold, P. B. Kelly, T. Tipton, and D. K. Veirs, J. Chem. Phys. **76**, 57 (1982).
[3]R. A. Bernheim, L. P. Gold, P. B. Kelly, C. Tomczyk, and D. K. Veirs, J. Chem. Phys. **74**, 3249 (1981).
[4]R. A. Bernheim, L. P. Gold, P. B. Kelly, T. Tipton, and D. K. Veirs, J. Chem. Phys. **74**, 2749 (1981).
[5]R. A. Bernheim, L. P. Gold, and T. Tipton, J. Chem. Phys. **78**, 3635 (1983).
[6]K. P. Huber and G. Herzberg, *Constants of Diatomic Molecules* (Van Nostrand, New York, 1979).
[7]L. Wolniewicz and K. Dressler, J. Mol. Spectrosc. **67**, 416 (1977).
[8]J. Vergès, C. Effantin, J. d'Incan, D. L. Cooper, and R. F. Barrow, Phys. Rev. Lett. **53**, 46 (1984).
[9]D. L. Cooper, R. F. Barrow, J. Vergès, C. Effantin, and J. d'Incan, Can. J. Phys. **62**, 1543 (1984).
[10]D. D. Konowalow and J. L. Fish, J. Chem. Phys. **76**, 4571 (1982).
[11]D. D. Konowalow and J. L. Fish, Chem. Phys. **84**, 463 (1984).
[12]I. Schmidt-Mink, W. Müller, and W. Meyer, Chem. Phys. **92**, 263 (1985).
[13]C. A. Tomczyk, Dissertation, The Pennsylvania State University, 1984, University Park, Pa.
[14]W. M. Kosman and J. Hinze, J. Mol. Spectrosc. **56**, 93 (1975).
[15]C. R. Vidal and H. Scheingraber, J. Mol. Spectrosc. **65**, 46 (1977).
[16]C. R. Vidal, Comm. At. Mol. Phys. **17**, 173 (1986).
[17]C. R. Vidal and W. C. Stwalley, J. Chem. Phys. **77**, 883 (1982).
[18]C. R. Vidal and W. C. Stwalley, J. Chem. Phys. **80**, 2697 (1984).
[19]P. Kusch and M. M. Hessel, J. Chem. Phys. **67**, 586 (1977).
[20]J. G. Balz, R. A. Bernheim, L. P. Gold, and T. Linn, Comput. Chem. **9**, 53 (1985).
[21]G. Herzberg, *Molecular Spectra and Molecular Structure. I. Spectra of Diatomic Molecules* (Van Nostrand, New York, 1950).
[22]See AIP document no. PAPS JCPSA-87 0861-69 for 69 pages of the term values of the $E\,^1\Sigma_g^+$ state. Order by PAPS number and journal reference from American Institute of Physics, Physics Auxiliary Publication Service, 335 East 45th Street, New York, NY 10017. The price is $1.50 for each microfiche (98 pages) or $5.00 for photocopies of up to 30 pages, and $0.15 for each additional page over 30 pages. Airmail additional. Make check payable to the American Institue of Physics.
[23]D. L. Albritton, A. L. Schmeltekopf, and R. N. Zare, in *Molecular Spectroscopy: Modern Research*, edited by K. N. Rao (Academic, New York, 1976), Vol. II.
[24]J. H. Ahlberg, E. N. Nilson, and J. L. Walsh, *The Theory of Splines and Their Application* (Academic, New York, 1967).
[25]P. Senn, P. Quadrelli, K. Dressler, and G. Herzberg, J. Chem. Phys. **83**, 962 (1985).
[26]K. Dressler, R. Gallusser, P. Quadrelli, and L. Wolniewicz, J. Mol. Spectrosc. **75**, 205 (1979).
[27]K. Dressler, in *Photophysics and Photochemistry above 6 eV*, edited by F. Lahamani (Elsevier, Amsterdam, 1985).
[28]D. M. Bishop and L. M. Cheung, J. Chem. Phys. **78**, 1396 (1983).
[29]D. M. Bishop and L. M. Cheung, J. Chem. Phys. **78**, 7265 (1983).
[30]C. R. Vidal, Chem. Phys. Lett. **65**, 81 (1979).
[31]M. Glass-Maujean, P. Quadrelli, and K. Dressler, J. Chem. Phys. **80**, 4355 (1984).